



ELSEVIER

Contents lists available at SciVerse ScienceDirect

Measurement

journal homepage: www.elsevier.com/locate/measurement

Calibration and analysis of eccentric error of the laser rotary-scanning measurement system

Tung-Hsien Tsai^{a,*}, Kuang-Chao Fan^b^a Dept. of Mechanical Engineering, Hsiuping University of Science and Technology, 11, Gungye Rd., Dali Dist., Taichung, Taiwan, ROC^b Dept. of Mechanical Engineering, National Taiwan University, 1, Roosevelt Rd., Sec. 4, Taipei, Taiwan, ROC

ARTICLE INFO

Article history:

Received 23 November 2010

Received in revised form 5 September 2011

Accepted 10 October 2011

Available online 19 October 2011

Keywords:

360° profile measurement

Alignment errors

Calibration

Non-contact measurement

ABSTRACT

A laser rotary-scanning measurement system was developed for the reverse engineering of 360° objects. The system is constructed by an optical head and a rotary indexing. The optical head is composed of a laser diode strip-light projector and dual CCD cameras. Based on the principle of structured-light triangulation, a laser line is projected onto the object upon which the distorted line is captured by dual CCD cameras from left and right simultaneously. By processing a series of line fittings from the discrete angular positions of an object, the entire 3D profile can be reconstructed. Since the actual space coordinates of the object are computed according to the geometric relationship between the coordinate of optical head system and the coordinate of the rotary indexing systems, if these two coordinate systems are not in good alignment, errors in the computed coordinates will be introduced.

This paper describes the influences of the alignment and eccentricity errors of the laser rotary-scanning measurement system on the computed geometrical profile. Calibration procedures are then proposed to adjust the alignment to avoid image distortions and thus enhance the system accuracy. Experimental results show that this easy-to-use calibration procedure can significantly improve the accuracy of the system.

© 2011 Elsevier Ltd. All rights reserved.

1. Introduction

In general, the 3D surface profile of an object can be acquired by using a non-contact laser scanning measurement system [1–3]. However, when measuring an object that has a large surface, large curvature, or a full 360° profile, one can acquire only one set of sectional measurement points in each measurement. For reconstructing the entire object, every set of sectional measurement points acquired at different positions must match with one another [4–8]. Therefore, the optimal shape error analysis for the matching images of the same area for two sets of sectional measurement surfaces is desired. In practice; however, this is tedious and time consuming.

For a smooth object having 360° shape, e.g., circular shaft, human sculpture or club head, one can acquire the entire profile through line-by-line increments using a rotary measurement system. Chang proposed a neural network algorithm to measure a 360° profile of an object [9]. Using the laser rotary-scanning measurement system, the processes of sectional scanning and image matching as described above can be avoided. Measurement time can also be saved. But the coordinates of this measurement system must be calibrated to avoid image distortions, and thus to enhance the system accuracy. In this paper, we proposed an easy-to-use calibration procedure to solve this problem and to adjust the alignment to avoid image distortions.

The schematic diagram of a laser rotary-scanning measurement system is illustrated in Fig. 1. The coordinate system of the laser rotary-scanning measurement is an actual space coordinate system (X,Y,Z); the original point of actual space coordinate system coincides with the center of

* Corresponding author. Tel.: +886 4 24961100; fax: +886 4 24961535.

E-mail addresses: tonytsai@mail.hust.edu.tw (T.-H. Tsai), fan@ccms.ntu.edu.tw (K.-C. Fan).

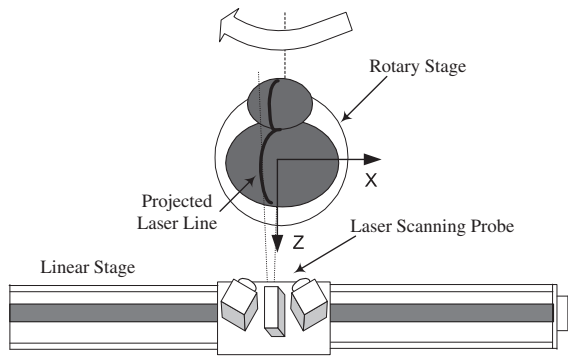


Fig. 1. Schematic diagram of a laser rotary-scanning measurement system.

the rotary table, and the direction of Y-axis is outward from the paper. The laser scanning probe projects a strip-light onto the object. A CCD camera can then capture the image of the deformed line. The coordinates of the deformed images could be transformed into the related space coordinates of the object according to the mapping function, which is acquired by using a pre-calibration procedure. By processing a series of laser strip images from the discrete angular positions of an object, the entire 3D profile can be reconstructed. Discussions on the alignment errors and accuracy calibration issues for this measurement system have not been found in any literature yet. In this paper, we investigate the errors of a laser rotary-scanning measurement system and propose a calibration procedure for the measurement system to improve its measuring accuracy.

2. The geometric principles of the rotary measurement system

Fig. 2 shows the geometric relationship of the rotary measurement system. The Y-axis direction is outward from the paper. Let $P(x, y, z)$ be a point of the object in the actual space coordinates, and $O(0, 0, 0)$ be the center of this actual space coordinates. Angle θ is the clockwise rotation angle of the rotary table of each step. The value (y', z') indicates the computed coordinate for a point on the section line, which is a line on the Y–Z plane that crosses the object, and there x' equals zero. Each deformed image that the CCD captures indicates the information of a section line.

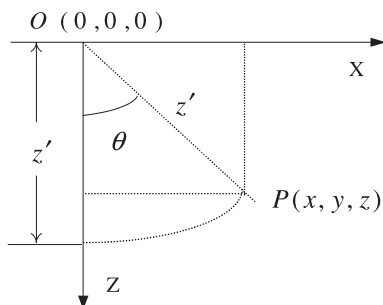


Fig. 2. The geometric principles of a rotary measurement system.

According to the mapping function, we can calculate the computed space coordinates of the section line, but they are not the actual space coordinates of the object. For acquiring the actual space coordinates, the computed space coordinates (y', z') must be transformed into the actual space coordinates $P(x, y, z)$. The geometric relationship between the rotary position and the space coordinate must be considered. The transformation equations of the computed coordinate (y', z') and the actual space coordinate $P(x, y, z)$ are shown as follows:

$$\begin{cases} x = z' \sin \theta \\ y = y' \\ z = z' \cos \theta \end{cases} \quad (1)$$

From Eq. (1), the actual space coordinates of the object are determined according to a trigonometric function. The accuracy of the actual space coordinates $P(x, y, z)$ depend on the geometric relationship between the laser rotary-scanning measurement system and the rotary system. If these coordinate systems do not coincide, errors of computed coordinate would be obtained from Eq. (1).

3. Error analysis of the coordinate system deviations

From the above descriptions, the actual space coordinates of the object can be determined by using Eq. (1). Here, we assume that the position of the center of the rotary table is located exactly at the center of the actual space coordinates, and the normal direction of the rotary table coincides with the Y-axis of the actual space coordinates. In practice, these two assumptions are not always satisfactory. There exist a few physical deviations between the rotary system and the actual space coordinate system. These deviations will induce computing errors.

3.1. The error caused by the inclined axis of the rotary table

For simplicity of descriptions, the analysis of the error caused by the inclined angle of the rotary table will be divided into two special conditions. One is that the axis of the rotary table exactly lies on the X–Y plane of the actual space coordinates but has an inclined angle β with respect to Y-axis. The other is that the axis of the rotary table exactly lies on the Y–Z plane of the actual space coordinates but has an inclined angle γ with respect to Y-axis. The transformation equations of two special conditions are described respectively as follows.

If the axis of the rotary table exactly lies on the X–Y plane of the actual space coordinates but has an inclined angle β with respect to Y-axis, the coordinate system XYZ is rotated through an inclined angle β about Z axis. The new coordinate system can be defined as $X_{\beta}^* Y_{\beta}^* Z_{\beta}^*$. The rotation matrix can be written as M_{β} . The measured point $(0, y', z')$ is rotated about the axis of the rotary table (Y_{β}^*) through an angle θ to a new position. The rotation matrix can be written as $(M_{\theta})_{\beta}$. The inclined coordinate system $X_{\beta}^* Y_{\beta}^* Z_{\beta}^*$ is returned to the original XYZ coordinate system by the inverse matrix M_{β}^{-1} . Then the transformation equations of the computed coordinate $(0, y', z')$ and the actual space coordinate $P(x, y, z)$ are shown as follows:

$$\begin{bmatrix} x \\ y \\ z \end{bmatrix} = M_{\beta}^{-1}(M_{\beta})_{\theta}M_{\beta} \begin{bmatrix} 0 \\ y' \\ z' \end{bmatrix} \quad (2)$$

where

$$M_{\beta}^{-1} = \begin{bmatrix} \cos \beta & \sin \beta & 0 \\ -\sin \beta & \cos \beta & 0 \\ 0 & 0 & 1 \end{bmatrix}, (M_{\beta})_{\theta} = \begin{bmatrix} \cos \theta & 0 & \sin \theta \\ 0 & 1 & 0 \\ -\sin \theta & 0 & \cos \theta \end{bmatrix},$$

$$M_{\beta}^{-1} = \begin{bmatrix} \cos \beta & -\sin \beta & 0 \\ \sin \beta & \cos \beta & 0 \\ 0 & 0 & 1 \end{bmatrix} \quad (3)$$

Therefore, when we substitute the rotation matrices M_{β} , $(M_{\beta})_{\theta}$ and M_{β}^{-1} into Eq. (2), the transformation equations of the computed coordinate can be acquired by

$$\begin{cases} x = y' \cos \beta \sin \theta + z' \cos \beta \sin \theta \\ y = y'(\sin^2 \beta \cos \theta + \cos^2 \beta) + z' \sin \beta \sin \theta \\ z = -y' \sin \beta \sin \theta + z' \cos \theta \end{cases} \quad (4)$$

Furthermore, if the axis of the rotary table exactly lies on the Y–Z plane of the actual space coordinates but has an inclined angle γ with respect to Y-axis. Similar to the description as above, the coordinate system XYZ is rotated through an inclined angle γ about Y axis. The new coordinate system can be defined as $X_{\gamma}^*Y_{\gamma}^*Z_{\gamma}^*$. The rotation matrix can be written as M_{γ} . The measured point $(0, y', z')$ is rotated about the axis of the rotary table (Y_{γ}^*) through an angle θ to a new position. The rotation matrix can be written as $(M_{\gamma})_{\theta}$. The inclined coordinate system $X_{\gamma}^*Y_{\gamma}^*Z_{\gamma}^*$ is returned to the original XYZ coordinate system by the inverse matrix M_{γ}^{-1} . Then the transformation equations of the computed coordinate $(0, y', z')$ and the actual space coordinate $P(x, y, z)$ are shown as follows:

$$\begin{bmatrix} x \\ y \\ z \end{bmatrix} = M_{\gamma}^{-1}(M_{\gamma})_{\theta}M_{\gamma} \begin{bmatrix} 0 \\ y' \\ z' \end{bmatrix} \quad (5)$$

where

$$M_{\gamma}^{-1} = \begin{bmatrix} 1 & 0 & 0 \\ 0 & \cos \gamma & \sin \gamma \\ 0 & -\sin \gamma & \cos \gamma \end{bmatrix}, (M_{\gamma})_{\theta} = \begin{bmatrix} \cos \theta & 0 & \sin \theta \\ 0 & 1 & 0 \\ -\sin \theta & 0 & \cos \theta \end{bmatrix},$$

$$M_{\gamma}^{-1} = \begin{bmatrix} 1 & 0 & 0 \\ 0 & \cos \gamma & \sin \gamma \\ 0 & -\sin \gamma & \cos \gamma \end{bmatrix} \quad (6)$$

Therefore, when we substitute the rotation matrices M_{γ} , $(M_{\gamma})_{\theta}$ and M_{γ}^{-1} into Eq. (4), the transformation equations of the computed coordinate can be acquired by

$$\begin{cases} x = -y' \sin \gamma \sin \theta + z' \cos \gamma \sin \theta \\ y = y'(\sin^2 \gamma \cos \theta + \cos^2 \gamma) + z' \cos \gamma \sin \gamma(1 - \cos \theta) \\ z = y' \cos \gamma \sin \gamma(1 - \cos \theta) + z'(\sin^2 \gamma + \cos^2 \gamma \cos \theta) \end{cases} \quad (7)$$

Briefly, the actual space coordinate $P(x, y, z)$ depends upon the point position of the object (y', z') and the inclined angle of the axis of the rotary table (β, γ) . In fact, if the axis of the rotary table neither lies on the X–Y plane

nor on the Y–Z plane of the actual space coordinates and has an inclined angle with respect to Y-axis. The transformation equations of the computed coordinate (y', z') and the actual space coordinate $P(x, y, z)$ will be more complicated. Under different inclined conditions of the axis of the rotary table, the transformation equations of the actual space coordinates are different.

Of course, the inclined angle can be obtained by appropriate measurement equipments, and then it can be calibrated. However, some measurement equipments are needed to measure inclined angle, and a calibration procedure is also needed to complete the calibration. This work is tedious and time consuming. In this paper, we proposed an easy-to-use calibration procedure to solve this problem and to adjust the alignment to avoid image distortions.

3.2. The error caused by the eccentricity of the rotary center

Fig. 3 shows the case that the center of the rotary table is not located exactly at the center of the actual space coordinates $O(0, 0, 0)$. In Fig. 3, the coordinate system of the laser rotary-scanning measurement is actual space coordinate system (X, Y, Z) , and (X^*, Y^*, Z^*) is the coordinate system of the center of the rotary table. While the direction of Y or Y^* axis is outward from the paper. Let $Q(x, y, z)$ be an actual space coordinate of the object, and $P(x, y, z)$ is a computed space coordinate according to the measured point $R(0, y', z')$. While (d_x, d_z) indicates the eccentricity of the center of the rotary table in the X and Z direction, respectively. From Fig. 3, the actual space coordinate $Q(x, y, z)$ can be determined as follows:

$$Q(x, y, z) \begin{cases} x = L' \sin(\theta - \alpha) + d_x \\ y = y' \\ z = L' \cos(\theta - \alpha) + d_z \end{cases} \quad (8)$$

According to the measured value (y', z') , the computed coordinate $p(x, y, z)$ can be acquired by

$$P(x, y, z) \begin{cases} x = (L + d_z) \sin \theta \\ y = y' \\ z = (L + d_z) \cos \theta \end{cases} \quad (9)$$

where $L' = L / \cos \alpha$. Then the eccentric errors E_x and E_z between the actual space coordinate and computed coordinate in the X and Z directions are:

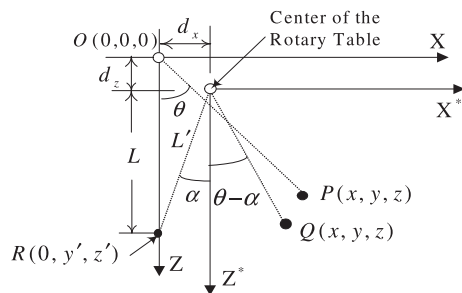


Fig. 3. The center of the rotary table deviations.

$$\begin{aligned} E_x &= (L + d_z) \sin \theta - [L' \sin(\theta - \alpha) + d_x] \\ &= d_z \sin \theta + d_x(\cos \theta - 1) \end{aligned} \quad (10)$$

$$\begin{aligned} E_z &= (L + d_z) \cos \theta - [L' \cos(\theta - \alpha) + d_z] \\ &= -d_x \sin \theta + d_z(\cos \theta - 1) \end{aligned} \quad (11)$$

Eqs. (8) and (9) can be rewritten as:

$$\begin{aligned} E_x &= R \sin(\theta + \phi) - d_x \\ E_z &= R \cos(\theta + \phi) - d_z \end{aligned} \quad (12)$$

where $\tan \phi = d_x/d_z$, and $R = \sqrt{d_x^2 + d_z^2}$.

If translates the computed coordinate with distance (d_x, d_z), then Eq. (10) would be changed to:

$$\begin{aligned} E'_x &= R \sin(\theta + \phi) \\ E'_z &= R \cos(\theta + \phi) \end{aligned} \quad (13)$$

And

$$E_x'^2 + E_z'^2 = R^2 \quad (14)$$

From Eq. (11), we can see that each point of the object on the X-Z plane has the same distance error to the center of the rotary table. Due to the deviations in the center of the rotary table (d_x, d_z), the object profile will expand or shrink its geometrical shape. A measurement error will be induced causing deviations in the center or incline axis system. The causes of this measurement error are due to d_x, d_z and the inclined angles of the system. Therefore, the measurement system should be calibrated to improve the measurement accuracy.

4. The calibration principle and procedures for rotary measurement system

Measurement errors are caused by the eccentricity and the inclined angles of the center of the rotary table. The relationships between these error terms are non-linear. It is difficult to acquire each error term in a simple and efficient manner. Here, we propose a simple calibration procedure to enhance the accuracy of the system. The calibration procedure is divided into two steps. The first step is the inclination calibration and the second the eccentricity calibration. The flow chart of the calibration procedure is shown in Fig. 4. The calibration procedure will be described in detail from Section 4.1 to Section 4.2.

4.1. Inclination calibration

The laser scanning probe projects a vertical laser strip onto the object. Since the Y-axis of the space coordinate is defined in the vertical direction. For calibrating the normal direction of the rotary plane coincident to the Y-axis, a leveling adjustment is executed alternately with two perpendicular directions for the laser scanning probe and the rotary table planes until they are within 1 arcsec tolerance using an electronic level. Therefore, the problem of determining the system inclined angle can be solved in a simple and efficient way by using the inclination calibration as shown here.

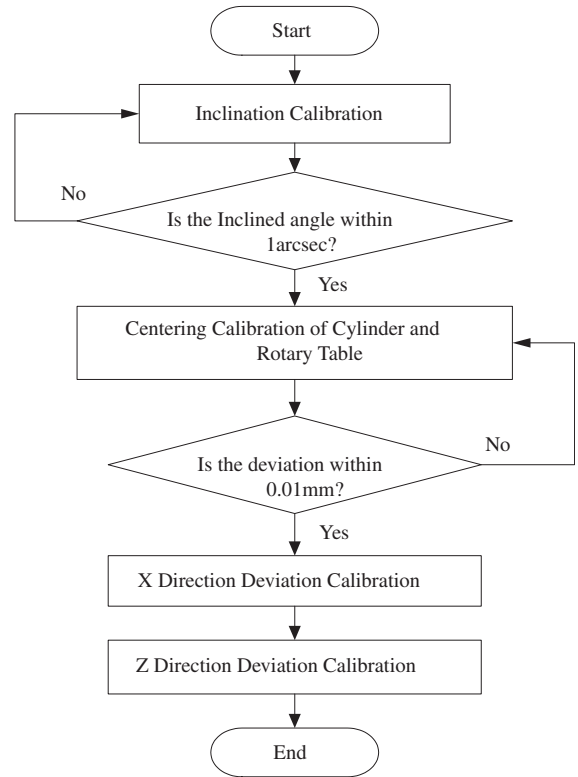


Fig. 4. The flow chart of the calibration procedure.

4.2. Eccentricity calibration

After completing the inclination calibration, a cylinder with known radius R is adopted to test the eccentricity of the center position of the rotary indexing. The procedure is described as follows:

4.2.1. The centering calibration of cylinder and rotary table

As shown in Fig. 5, the cylinder is placed in the center of the rotary table. A dial indicator with $1 \mu\text{m}$ resolution touches the cylinder at A and resets in the X direction. The rotary table then rotates 180° and the cylinder is adjusted one half of the deviation indicated on the dial indicator along the inverse direction. The procedure is repeated until the deviation is within 0.01 mm tolerance. And then, the calibration procedure of Z direction is the same as the calibration procedure of X direction.

4.2.2. X direction deviation calibration

When the center of the cylinder coincides with the center of the rotary table, the center position of the rotary table can be determined easily by scanning the cylinder and using the laser scanning probe. The laser scanning probe scans the cylinder linearly from left to right with a pitch of 1 mm along the X direction, as shown in Fig. 6. However, in this calibration procedure, the scan data are limited to a small and short arc, so if we use these measurement data to fit the circle equation of the cylinder cross-section arc directly, the curve fitting error will be very large and the

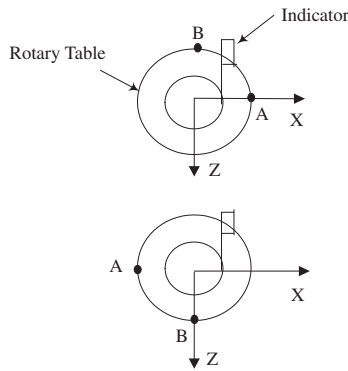


Fig. 5. The schematic diagram for the cylinder rotary table calibration method.

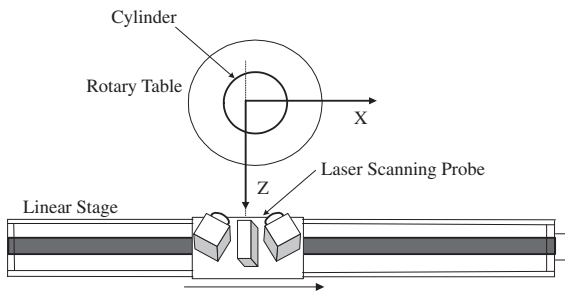


Fig. 6. Schematic diagram for calibration X direction deviation.

calibration accuracy of X-direction deviation will not be good enough. Since the scan data is only required to find the vertex of the curve and the vertex vicinity of the polynomial fitting curve coincides with the circular curve. Therefore, we use a polynomial approximation to fit the circle curve for calibrating the X-direction deviation. Let the initial position be $x = 0$, and then a set of the average \bar{z} values and the corresponding x value of each step can be acquired. Because the equation of a circle is a polynomial function of order 2, therefore, a polynomial function of order 2: $\bar{z} = ax_i^2 + bx_i + c$ can be used to fit the cylinder cross-section arc. If the least-squares method is used, the coefficient of curve fitting functions a–c can be determined. Therefore, the vertex of the polynomial function is located at $x = -b/2a$. Fig. 7 shows the schematic diagram of polynomial curve fitting for calibration X direction deviation. Since the vertex vicinity of the polynomial fitting curve coincides with the circular curve, and the center of the rotary table passes through the vertex of the polynomial fitting curve, moving the laser scanning probe to the vertex position ($x = -b/2a$) will initiate the X direction deviation calibration. Briefly, the X-direction deviation is obtained by using curve fitting method, and then the accuracy will be higher than that by calibrating the radius error of cylinder directly.

4.2.3. Z direction deviation calibration

Since the projected laser line passes through the center of the rotary table and coincides with the normal direction

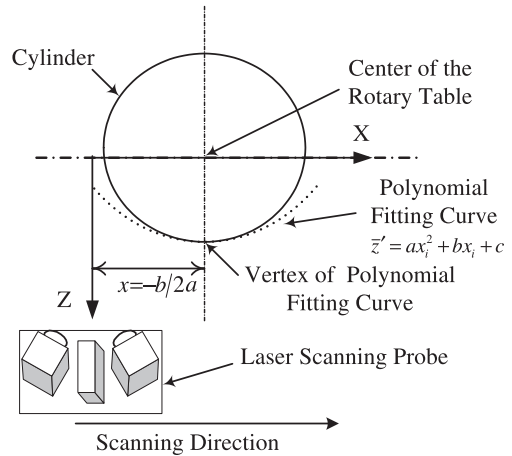


Fig. 7. Schematic diagram of polynomial curve fitting for calibration X direction deviation.

of the rotary table plane, the deviation of d_z can be determined by measuring the average value \bar{z} of the cylinder on the Y–Z plane. The deviation is then equal to the product from subtracting the radius of the cylinder from \bar{z} . If the deviation “ d_z ” is positive, then the rotary table is moved back by d_z . Inversely, the rotary table is moved forward by d_z and the measurement system calibration is completed.

5. The practice of calibration and experimental results

In this paper, the scanning head of this laser rotary-scanning measurement system adopts a laser diode projector and dual CCD cameras attached with an OPTEM ZOOM 70 with a $0.38\times$ TV tube and $0.25\times$ auxiliary lens. This optical scanning probe is mounted on a linear stage to execute line scanning measurement. The resolution of CCD camera is 768×494 picture element [8]. Table 1 lists the specifications of this system performance. Experimental measurement results show that the system accuracy is about 0.05 mm and 0.06 mm in the Y-axis and Z-axis direction at the original focus position respectively.

To investigate the calibration procedure of measurement system, we adopted a cylinder that has a radius of 26.930 mm to execute the calibration procedure. The inclination calibration and cylinder centering are executed first. The cylinder is then scanned from left to right with a pitch of 1 mm and the vertex position of the polynomial function is calculated by using the least-squares method. The result of vertex position was 14.25 mm and then the laser scanning probe was moved by 14.25 mm along the X-axis

Table 1
Scanning head specifications of measurement system.

	Lowest	Highest
Magnification	0.071×	0.50×
Field of view	67.4 mm × 89.8 mm	9.5 mm × 12.6 mm
Depth of field	30 mm	2.7 mm
Working distance	350 mm	350 mm

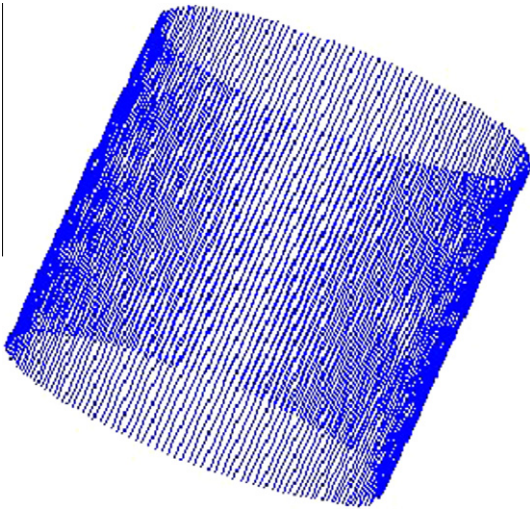


Fig. 8. The line segments of the measured data for the cylinder.



Fig. 9. The prototype picture of a marmot toy.

direction to finish the X direction calibration. Next, measure the average distance \bar{z} of the cylinder. The result was 27.346 mm and the deviation of d_z was 0.416 mm. Because d_z was positive, the rotary table is moved back by 0.416 mm and the average distance of the cylinder is measured again. The result was 26.941 mm, and the radius error was 0.011 mm. Since the accuracy of this laser rotary-scanning measurement system is 0.05 mm. Therefore, the calibration procedure has now been accomplished.

Using a measurement system calibrated to scan the cylinder with a rotation angle of 2° per step of the rotary table, the total number of scanned lines was 180. Fig. 8 shows the line segments of the measured data. The result of the measured diameter for the cylinder was 53.921 mm and the diameter error was 0.061 mm. This reveals that the calibration procedure we proposed works very well and the accuracy is satisfactory.

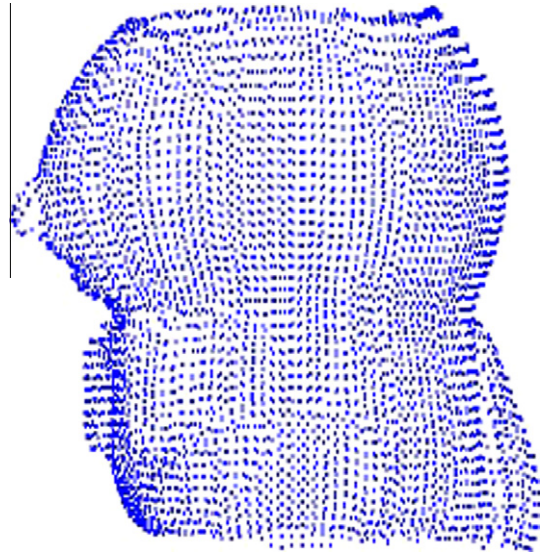


Fig. 10. The measured data from a toy using a rotary measurement system without calibration.

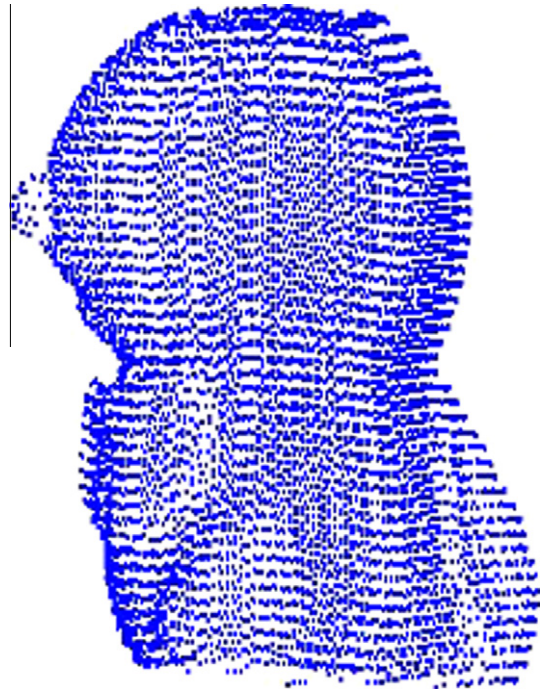


Fig. 11. The entire line segments from the measured data for the toy using a calibrated measurement system.

Subsequently, a marmot toy was measured by using a rotary measurement system without and with calibration, respectively. Fig. 9 shows a prototype picture of a marmot toy. Fig. 10 presents the set of measured data using a rotary measurement system without calibration. From Fig. 10, if the measurement system is not calibrated, it apparently reveals an enlargement distortion of the object compared to the prototype. However, the marmot toy was measured

by using the calibrated measurement system. The entire line segments of the measured data are shown in Fig. 11. From Fig. 11, if the measurement system is calibrated, the set of measured data is more accurate in comparison with the measured data without calibration (Fig. 10).

6. Conclusion

A laser scanning probe can be used to project structured-light onto an object to allow image capture by a CCD camera. By processing a series of laser strip images from the discrete angular positions of an object, the entire 3D profile can be reconstructed. This measurement system is convenient and easy to operate. The measured data depends on the geometric relationship between the measurement and rotary systems. For acquiring reliable measured data, the measurement system must be calibrated.

In this paper, we describe the errors from a laser rotary-scanning measurement system that are induced by the deviations in the rotary table coordinates. From the error analysis descriptions, for different alignment or eccentricity errors of the axis of the rotary table, the transformation equations of the actual space coordinates are different. Unfortunately the alignment errors of the axis of the rotary table are unknown, and the causes for these deviations are so complex that one cannot determine all of the causes by using a simple method or procedure. To eliminate the

deviations simply and improve the measurement accuracy efficiently, we proposed a calibration procedure for adjusting the coordinate alignment and the eccentricity of the rotary center separately. Experimental results show that this calibration procedure can be easily executed. The deviations can be acquired and adjusted and the accuracy of the system can be improved.

References

- [1] K.C. Fan, A non-contact automatic measurement for free-form surface profile, *Comput. Int. Manuf. Syst.* 10 (4) (1997) 277–285.
- [2] C.C. Ho, 3D Surface Matching Techniques in Image Measurements, Master Thesis, National Taiwan University, 1997.
- [3] S. Igarashi, K. Shibukawa, K. Takeuchi, 3D Measurement of shape by projection method using special grating pattern, *Int. J. Jpn. Soc. Prec. Eng.* 26 (2) (1992) 128–133.
- [4] P.J. Besl, A method for registration of 3D shapes, *IEEE Trans. PAMI* 14 (2) (1992) 239–256.
- [5] Y. Chen, G. Medion, Object modeling by registration of multiple range images, *Image Vis. Comput.* 10 (3) (1992) 145–155.
- [6] D.W. Eggert, A.W. Fitzgibbon, R.B. Fisher, Simultaneous registration of multiple range views for use in reverse engineering of CAD models, *Comput. Vis. Image Und.* 69 (3) (1998) 253–272.
- [7] K.C. Fan, T.H. Tsai, Optimal shape error analysis of the matching image for a free-form surface, *Int. J. Robot. Comput.-Int. Manuf.* 17 (3) (2001) 215–222.
- [8] T.H. Tsai, K.C. Fan, A variable resolution optical profile measurement system, *Meas. Sci. Technol.* 13 (2002) 190–197.
- [9] M. Chang, W.C. Tai, 360° profile noncontact measurement using a neural network, *Opt. Eng.* 34 (12) (1995) 3572–3575.